Materials Today Bio 23 (2023) 100824

Contents lists available at ScienceDirect

Materials Today Bio

journal homepage: www.journals.elsevier.com/materials-today-bio

Control of the growth and development of murine preantral follicles in a biomimetic ovary using a decellularized porcine scaffold

Eun young Park [a,1], Jin hee Park [a,1], Nhu Thi Quynh Mai [b], Byoung-San Moon [b,**], Jung Kyu Choi [a,*]

[a] Department of Biotechnology, College of Life and Applied Sciences, Yeungnam University, Gyeongsan, 38541, South Korea
[b] Department of Biotechnology, Chonnam National University, Yeosu, 59626, Republic of Korea

ARTICLE INFO

Keywords:
Decellularization technology
Biomimetic ovary
Ovarian follicle
Extracellular matrix

ABSTRACT

This study aimed to derive mature oocytes from murine preantral follicles cultured in a biomimetic ovary with a porcine scaffold using decellularization technology. We evaluated the DNA content and the presence of cell and extracellular matrix (ECM) components, including collagen, elastin, and glycosaminoglycans (GAGs), in decellularized (decell) porcine ovaries. The DNA content inthe decell ovarian tissues was approximately 94 % less than that in native tissues (66 ± 9.8 ng/mg vs. 1139 ± 269 ng/mg). Furthermore, the ECM component integrity was maintained in the decell ovarian tissue. The soluble collagen concentration of native ovarian tissue (native) was 195.34 ± 15.13 μg/mg (dry wt.), which was less than 878.6 ± 8.24 μg/mg for the decell ovarian tissue due to the loss of cellular mass. Hydrogels derived from decell porcine ovaries were prepared to develop an in vitro biomimetic ovary with appropriate ECM concentration (2–6 mg/mL). Scanning electron microscope (SEM) imagining revealed that the complex fiber network and porous structure were maintained in all groups treated with varying ECM concentration (2–6 mg/mL). Furthermore, rheometer analysis indicated that mechanical strength increased with ECM concentration in a dose-dependently. The preantral follicles cultured with 4 mg/mL ECM showed high rates of antral follicle (66 %) and mature oocyte (metaphase II) development (47 %). The preantral follicles cultured in a biomimetic ovary with a decell porcine scaffold showed a higher rate of antral follicle and mature oocytes than those cultured in other biomaterials such as collagen and Matrigel. In mature oocytes derived from antral follicles, meiotic spindles and nuclei were stained using a tubulin antibody and Hoechst, respectively. Two-cell embryos were developed from MII oocytes following parthenogenetic activation. Preantral follicles were cultured in a biomimetic ovary derived from the ECM of a decell porcine ovary, and embryos were generated from MII oocytes. This biomimetic ovary could contribute to restoring fertility in infertile women with reduced ovarian function, benefit mating efforts for endangered species, and maintain animals with valuable genetic traits.

1. Introduction

The ovarian follicle is the smallest structural and functional tissue unit constituting the mammalian ovary and can generate one egg via folliculogenesis. In humans, females are born with approximately one million follicles that never regenerate and undergo degeneration over time [1,2]. Less than 1 % of these follicles are used ina female's reproductive life until menopause, while the rest are destined for degeneration and are never involved in egg production. Therefore, it is necessary to culture ovarian follicles destined for in vivo degeneration to obtain large numbers of fertilizable eggs [3]. This can contribute to restoring fertility in women later in life, or whose ovarian function has reduced due to radiation or chemotherapy.

Mammalian ovaries are composed of a complex 3D structure with an extracellular matrix (ECM) composed of collagen, laminin, fibronectin, proteoglycan, and polysaccharides, which play vital roles in cell-cell interactions and communication for follicle formation, development, and migration within the ovary [4,5]. To mimic an in vivo-like

* Corresponding author.
** Corresponding author.
E-mail addresses: bsmoon@jnu.ac.kr (B.-S. Moon), jungkyuc@ynu.ac.kr (J.K. Choi).
[1] These authors contributed equally to this work.

https://doi.org/10.1016/j.mtbio.2023.100824
Received 14 July 2023; Received in revised form 22 September 2023; Accepted 28 September 2023
Available online 7 October 2023

microenvironment for in vitro follicle culture, it is necessary to introduce a 3D culture system combined with the ECM, compared to a 2D culture with a flat surface of a culture dish in which the 3D structure of the follicle is not created in vitro. Thus, ovarian follicles have been cultured in a 3D culture system using various biomaterials, such as alginate [6], collagen [7], fibrin gel [8], and polyethylene glycol [9–11], alone or in combination, to recreate the ECM microenvironment in the ovary. However, these methods do not accurately simulate the ovarian ECM microenvironment in vivo.

To overcome the limitations of existing biomaterials, a decellularized extracellular matrix (dECM), isolated by removing cells from ovarian tissues, has emerged as a new alternative for biomimetic ovaries [12,13]. Biomimetic ovaries have been created using ECM isolated from decellularized porcine ovaries, which are anatomically and physiologically similar to humans [14,15]. In this studyt, the presence of cells and ECM were confirmed using hematoxylin and eosin (H&E) and 4′,6-diamidino-2-phenylindole (DAPI) staining, DNA quantification, and histological analyses to confirm decellularization in porcine ovaries. A Sircol soluble collagen assay was used to estimate the soluble collagen content within the tissues, and hydrogels with different concentrations derived from decellularized porcine ovary were characterized based on themicrostructure and mechanical properties using scanning electron microscopy (SEM) and rheometer respectively. We observed in vitro growth and development of mouse preantral follicles in a biomimetic ovary with a decellularized porcine scaffold. For the first time, mature oocytes retrieved from the antral follicles were used to generate embryos after parthenogenetic activation. Biomimetic ovaries present a powerful tool for the in vitro culture of follicles for fertility preservation.

2. Methods

2.1. Decellularization of porcine ovary

Porcine ovaries for decellularization were obtained from a local slaughterhouse and transported to the laboratory in saline prewarmed at 39 °C. When decellularization was performed using 100 mL of decellularization solution, the cortex area of approximately 30–50 ovaries was used because it was sufficiently submerged. After washing the samples once with saline, only the cortex of ovaries (n = 30–50), the outer part of ovarian tissues, was cut into small pieces using scissors and chopped into small pieces using a scalpel. The minced ovarian tissue pieces were washed twice with distilled water (DW) by stirring using a digital rocker at 50 rpm for 15 min, followed by an additional overnight wash in DW at 4 °C. Subsequently, tissues were stirred in prewarmed 0.05 % trypsin-EDTA solution (Welgene, LS 015-10) at 500 rpm for 1 h at 37 °C and rinsed twice with DW for 15 min at 50 rpm. The tissues were treated in a 0.69 % tris (hydroxymethyl) aminomethane (Sigma, 252859) and 2.5 mM sodium deoxycholate (SDC, Sigma, 30970) solution at 50 rpm for 24 h, then rinsed two times with DW at 50 rpm for 15 min and placed in DW overnight at 4 °C to remove residual surfactant. Next, the tissues were stirred in a 4 % ethyl alcohol (Sigma, E7023) solution for 2 h at 50 rpm, rinsed two times with DW for 15 min at 50 rpm. Finally, the treated tissues were transferred to DPBS supplemented with 1 % penicillin-streptomycin (Gibco, 15070063) for overnight incubation at 4 °C and rinsed twice with for 15 min at 50 rpm to remove residual detergent. The decellularized tissues were milled using a mortar and pestle in LN2 and lyophilized. ECM powder was stored at −56 °C.

2.2. ECM hydrogel preparation

ECM powder was solubilized by adding 0.1 g of pepsin from porcine gastric mucosa (Sigma, P7012) to 100 mL of 0.01 N HCl solution per 1 g of ovarian ECM powder, followed by stirring at 500 rpm for 48 h at room temperature (RT). The solubilized ECM solution was filtered through a 40 μm cell strainer, generating ECM pre-gel solution with a concentration of 10 mg/mL, which was stored in a −56 °C freezer. ECM hydrogel gelation was performed by diluting ECM pre-gel solution to the desired concentration in a solvent composed of 10X PBS (1/9 of the pre-gel volume), 0.1 N NaOH (1/10 of the pre-gel volume) and DPBS, followed by suspending and mixing well using a vortex mixer. Gelation of the hydrogel was induced by incubating at 37 °C for 30 min.

2.3. DNA quantification

Residual DNA content of ovarian tissue (Native) and decellularized ovarian tissue (Decell) was extracted using a DNeasy Blood and Tissue kit (Qiagen, Germany) according to the manufacturer's instructions using 10–25 mg of tissue. Briefly, Native and Decell tissues were treated with Protease K (n = 6) at 56 °C until the tissue was completely lysed. DNA was extracted using the spin column method and quantified utilizing BioSpec-nano (Shimazu, Kyoto, Japan). The average of total DNA per mass of ECM power (ng/mg) was calculated.

2.4. Histological analysis

To assess the efficiency of nucleic materials removal of the Decell, we performed hematoxylin and eosin (H&E) and 4,6-diamino-2-phenylindole (DAPI) staining. Briefly, native and decell samples were fixed during 6 h at RT in 4 % (v/v) paraformaldehyde (PFA) and subsequently washed with PBS to make paraffin block. The samples were sectioned at 5 μm thick using a rotary microtome (Leica RM2235, Davisburg, MI). To perform H&E staining, the deparaffinized samples were immersed in hematoxylin for 3 minutes, followed by a 5-minute rinse under running tap water to eliminate any residue. Subsequently, the slides were incubated with eosin for 2 minutes, followed by a 5-minute rinse with running tap water. After rehydrating process, samples were mounted using an aqueous mounting solution (DAKO, Carpinteria, CA, USA), followed by imaging for further analysis. For DAPI staining, rehydrated samples were incubated with DAPI for 5-minutes and washed with PBS. The images were captured using confocal microscopy (K1 Fluo, Nanoscope Systems lnc., Korea). These images are representative of samples obtained from a minimum of three independent experiments.

For the evaluation of matrix preservation, ECM components were analyzed with Masson's Trichrome staining (BIOGNOST, Zagreb, Crotia) for detection of collagen, Elastica van Gieson staining (BIOGNOST, Zagreb, Crotia) for elastic fibers, and Alcian blue staining (ScienCell Research Laboratory, CA, USA) for glycosaminoglycan (GAG). Deparaffinized samples on slides were stained following the manufacturer's protocol, rehydrated as previously described, and mounted for imaging.

2.5. Acid-/pepsin-soluble collagen quantification

The acid-/pepsin-soluble collagen content in the Decell and Native was measured using a Sircol soluble collagen assay kit (Biocolor, Carrickfergus, Northern Ireland). Sample were digested with 0.5 M acetic acid containing 1 % (w/v) pepsin (P7012, Sigma) for 24 h at RT. The collagen suspension was precipitated by centrifugation at 5000 rpm for 10 min. Relative absorbance was measured in a 96-well plate at 555 nm using a microplate reader. Soluble collagen concentrations of Decell and Native were determined from the standard curve and results are expressed in μg collagen/mg dry weight.

2.6. Scanning electron microscopy

The ultrastructure of the ovarian ECM hydrogel was imaged using SEM. ECM hydrogel specimens for SEM were prepared by referring to a previously published method [3]. Briefly, ECM pre-gel solution at 2, 4, and 6 mg/mL concentration of the ECM hydrogel on a slide glass was incubated for 30 min at 37 °C in 5 % CO_2 incubator to induce gelation. Next, they were fixed in cold 2.5 % (v/v) glutaraldehyde in DPBS for 24 h and washed three times with DPBS for 30 min. The hydrogel was dehydrated using an ethanol gradient (30 %, 50 %, 70 %, 90 % and 100

%) for 45 min each and finally immersed in 100 % alcohol at 4 °C overnight. Additionally, 100 % alcohol was replaced three times for 45 min and dried slowly at RT overnight. The specimen was coated with platinum using an ion sputter (E−1030, Hitachi, Tokyo, Japan) and imaged using scanning electron microscopy (Hitachi S-4800; Hitachi Medical Corporation, Tokyo, Japan). The SEM images were analyzed for fiber diameter and pore size of the hydrogel for each ECM concentration using the image J software. Fiber diameter was quantified by measuring 100 spots in each group (n = 3) with the algorithm [16,17]. Pore size was calculated by measuring the average size of 2000 spots randomly selected for each group (n = 3).

2.7. Rheology

Rheological analysis for each concentration of the ECM hydrogel was performed using an MCR-301 rheometer (Anton Paar, Hertford, UK). Pre-gel solutions of 2, 4, 6, and 8 mg/mL ECM concentrations were added between 25 mm parallel plates, and the gap distance between the plates was set to 0.5 mm. After sample loading, mineral oil was applied to the edge of the plate to prevent evaporation of the hydrogel. The time sweep (1 rad/s, 1 % strain) was performed for 30 min (n = 3) to measure the storage (G′) and loss (G″) modulus of the ECM hydrogel after inducing gelation of ECM hydrogel at 37 °C in 5 % CO_2 incubator for 30 min. The storage modulus (G′), loss modulus (G″), and dynamic modulus of elasticity (E) were calculated by substituting them correspondingly in the following equation: $E = \sqrt{G'^2 + G''^2}$ [7].

2.8. In vitro culture of preantral follicles in ECM hydrogel

All animal experiments were performed with the approval of the Institutional Animal Care and Use Committee (IACUC) at Yeungnam University. Two-week-old female ICR mice were purchased from DBL (Seoul, Korea) and euthanized by cervical dislocation to collect ovarian tissues. Secondary follicles (100–130 μm) were carefully isolated from mice using a 26-gauge needle, transferred to L-15 supplemented with 10 % FBS, and mechanically separated into single follicles. The ECM hydrogel was prepared in concentrations of 2, 4, and 6 mg/mL immediately before use, and placed on ice to prevent gelation until use. The collected preantral follicles were put into ECM pre-gel solution and 5 μl droplets were added to the wells in a 96 well plate. Then, ECM hydrogel was incubated for 30 min at 37 °C with 5 % CO_2 to induce gelation. After gelation, prewarmed IVC (in vitro culture) medium composed of MEM-α (Gibco, 32571-036) supplemented with 5 % FBS (Gibco, 16000044), 1 % ITS, and 100 mIU/ml FSH was cultured at 37 °C in 5 % CO_2 incubator for 9 days. After adding IVC medium on the next day, half of the IVC medium was replaced with fresh medium every other day. On days 0, 5, 7, and 9 of culture, follicles were observed under phase contrast microscope to measure the diameter of follicles. Two perpendicular follicle diameter measurements were performed for each follicle to calculate an average diameter, referring to the previously used method [18]. In addition, to confirm the viability of the antral follicle on day 9, live/dead staining was performed by adding 2 μg/mL Calcein-AM (Invitrogen, C1430) and 1 μg/mL propidium Iodide (PI) to the antral follicle from the 4 mg/mL ECM hydrogel and incubating it at 37 °C for 10 min. Antral follicles were observed using the CELENA® S Digital Imaging System (Logos Biosystems, Korea).

2.9. In vitro maturation (IVM) of antral follicles and developmental competence of MII oocytes

For IVM, antral follicles were triggered by exposure to 50mIU/mL human chorionic gonadotrophin (hCG), 5 ng/mL human epidermal growth factor (hEGF) at 37 °C in 5 % CO_2 incubator for 18 h. The ovulated Cumulus Oocyte Complexes (COCs) were treated to remove cumulus cells using0.2 % hyaluronidase and incubated them at 37 °C in 5 % CO_2 for 3 min. The remaining cumulus cells were removed by gentle pipetting and classified as GV (germinal vesicle), GVBD (germinal vesicle breakdown), and MII (metaphase II). Oocytes at the germinal vesicle (GV) stage were judged by the presence of a clear GV, GV breakdown (GVBD) oocytes were judged by the disappearance of the clear GV (Figs. S1A and B), and MII oocytes were judged by the disappearance of the clear GV (Figs. S1C and D) and the appearance of a characteristic first polar body. To confirm spindle and chromosome organization, ovulated MII oocytes were stained with alpha Tubulin Monoclonal Antibody (TU-01), FITC (Invitrogen, MA1-19581), and Hoechst 33342 (Invitrogen, H3570). Briefly, oocytes were transferred to 4 % paraformaldehyde, and fixed for 30 min at RT. Then, permeabilization was performed in 0.5 % triton-X for 20 min at RT, and blocking was done in PBS supplemented with 1 % BSA to prevent non-specific binding. Oocytes were transferred to DPBS supplemented with 0.05 % TWEEN 20, treated with alpha tubulin monoclonal antibody (Invitrogen, MA1-19581) (1:1000), and then treated at 4 °C overnight. The treated oocytes were visualized by staining with DAPI (1 μg/mL in DPBS) for 3 min at 37 °C in 5 % CO2 incubator and observing under a CELENA® S Digital Imaging System (Logos Biosystems, Korea).

2.10. In vitro culture of preantral follicles from various biomaterials

Matrigel (Corning, 356231)and collagen I (rat tail, Gibco, A1048301) were kept on ice until immediately before use to prevent gelation. Matrigel hydrogel was prepared by mixing Matrigel and IVC medium at a ratio of 1:2 collagen hydrogel (2.5 mg/mL) was prepared according to manufacturer's recommended protocol. Briefly, collagen solution was calculated as (final volume)*(desired concentration, mg/ml)/(collagen concentration indicated on the vial, mg/ml), (final volume) * 1/10 of 10X DPBS, and (collagen solution volume) * 0.025 of 1 N sodium hydroxide (NaOH) were added. The remaining part in the final volume was adjusted using DW. Preantral follicle isolation and culture were performed in the same way as ECM hydrogel.

2.11. Parthenogenetic activation

The MII oocytes derived from antral follicles were further assessed by their embryonic development following parthenogenetic activation using Ca2+-free KSOM supplemented with 10 mM SrCl2 and 5 μg/mL cytochalasin B for 4 h. The activated oocytes were cultured to observe embryonic development for 4–5 days in M16 medium at 37 °C in 5 % CO2 incubator.

2.12. Statistical analysis

The statistical analysis was performed with analysis of variance (ANOVA) and generalized linear model (GLM) to determine the p value between various groups. The difference was taken as significant when the p value was less than 0.05.

3. Results and discussion

The experimental process for achieving and applying a biomimetic ovary in vitro is briefly described in Fig. 1. As shown in Fig. 1a, a decellularization process is used to remove cells from the porcine ovaries to construct a biomimetic ovary. Following decellularization, substantially less DNA and ECM were present in the decellularized porcine ovary. The decellularized tissues were evaluated by H&E and DAPI staining, DNA quantification, and histological analysis. Subsequently, it was confirmed that ECM isolated from decellularized porcine ovaries (dPO) formed hydrogels at various concentrations (2, 4, and 6 mg/mL) at 37 °C. The dECM hydrogel of various concentration was characterized using SEM and rheological analysis (Fig. 1b). Finally, to determine the optimal biomimetic ovarian microenvironment, preantral follicles were cultured in dECM hydrogel at various concentrations, and mature

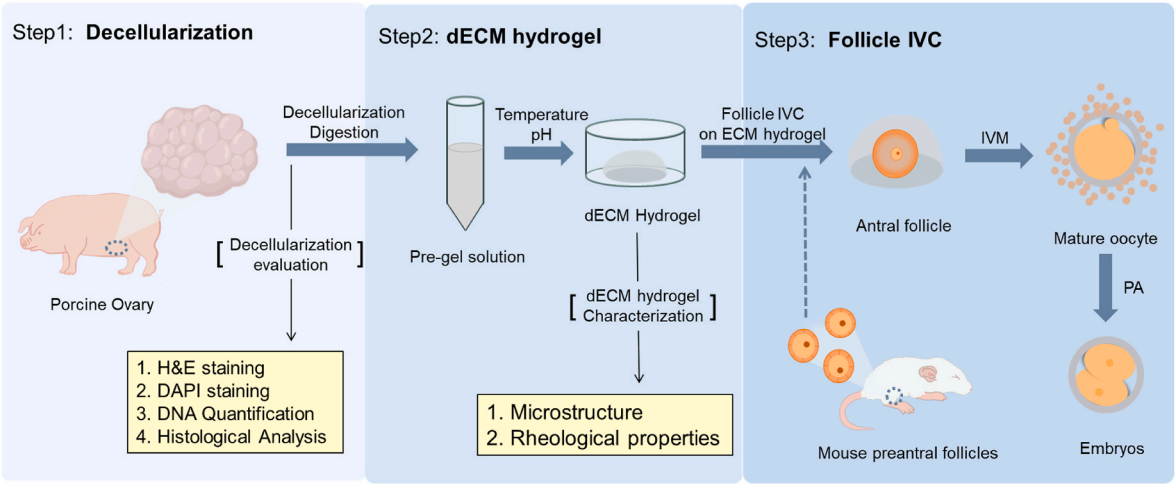

Fig. 1. Experimental approach. The experimental approach comprised decellularization, extracellular matrix (ECM) hydrogel preparation, and mouse secondary follicle in vitro culture (IVC). Porcine ovaries were decellularized with trypsin-EDTA, sodium deoxycholate (SDC), Tris, and alcohol. Decellularized tissues were evaluated by hematoxylin and eosin staining (H&E), 4′,6-diamidino-2-phenylindole (DAPI) staining, DNA quantification, and histological analysis. Subsequently, the tissues were milled into a fine powder in LN2, lyophilized, and enzymatically digested to prepare a decellularized ECM (dECM) pre-gel solution. The soluble matrix proteins in the pre-gel solution underwent self-assembly upon incubation at 37 °C for 30 min to form ovary-derived hydrogel for 3D culture. The dECM hydrogel was characterized using scanning electron microscopy (SEM) and rheological analysis. Preantral follicles were isolated from 2-week-old ICR mice, encapsulated in dECM hydrogel, and cultured for 9 days in vitro. Subsequently, MII oocytes derived from antral follicles were confirmed embryonic development using parthenogenetic activation.

oocytes derived from them developed into embryos following parthenogenetic activation (PA).

The dPO process is depicted in Fig. 2. Porcine ovaries were minced and the ECM was isolated by decellularization, lyophilization, and pepsin digestion. Finally, the ECM hydrogel formed at 37 °C for 30 min, where gelation was induced. We then determined DNA content and the presence of cell and ECM components, such as collagen, elastin, and GAGs, in decellularized porcine ovaries. The DNA content of decellularized ovarian tissues was significantly ($p < 0.05$) reduced by approximately 94.2 % compared to that of native tissues (1139 ± 269 ng/mg vs. 66 ± 9.8) (Fig. 3A). Histological analysis revealed a corresponding decrease in DAPI staining in the nucleus-stained area. Masson's trichrome staining (Fig. 4a, d), Elastica van Gieson (Fig. 4c, f), and Alcian blue staining (Fig. 4b, e) were performed. Collagen (blue), elastin fibers (black-blue), and GAGs (blue) were confirmed in both (native) and decellularized ovarian tissues (decell). Conclusively, we confirmed that the DNA content was successfully removed from the decellularized ovarian tissue, which showed that the integrity of ECM components, such as collagen, GAGs, and elastin, was maintained in the decellularized ovarian tissue.

In organs or tissues, collagen exists in both insoluble and soluble forms [19]. The majority of the ECM derived from decellularized ovaries consists of collagen [20]. To create collagen-based hydrogels from them in vitro, soluble collagen was utilized as it readily dissolves in water and forms a polymer network with a high water content, allowing for gel formation [21].

The Sircol soluble collagen assay was used to estimate the soluble collagen content within the tissues. The soluble collagen concentration of native ovarian tissue (native) was 195.34 ± 15.13 μg/mg (dry weight.), which was less than 878.6 ± 8.24 μg/mg for the decell (Fig. 5). In both native ovarian tissue and decellularized ovarian tissue, the amount of collagen present per milligram (mg) was measured. In the case of native tissue, cells and ECM coexist within the same unit area, while in decellularized ovarian tissue, most cells are removed during decellularization, resulting in a relatively higher proportion of ECM occupying the same unit area than native tissue [22]. Therefore, decellularized ovarian tissue exhibits a higher amount of soluble collagen, a constituent of the ECM, than native tissue. Most ovarian ECM is composed of collagen, which is distributed throughout the ovary [23]. Thus, we primarily quantified the amount of collagen, which is predominantly present in decellularized ovarian tissue, compared to other ECM components, such as GAGs and elastin. However, additional studies are required to identify other ECM components along with a number of unknown growth factors in the dECM to determine the mechanism by which they affect ovarian follicle growth and development.

We characterized the dECM hydrogels at various concentrations (2–6 mg/mL) using SEM imaging and rheological analysis. As shown in Fig. 6 (A and B), the mechanical properties, including both the storage (G, representing the elastic effect) and loss (G, representing the viscous effect) moduli, were measured using a rheometer according to the dECM concentration. As the dECM increased, the modulus tended to increase, confirming that the rheological properties of the dECM hydrogel were affected by the dECM concentration (Fig. 6A). The elastic moduli of 8.7

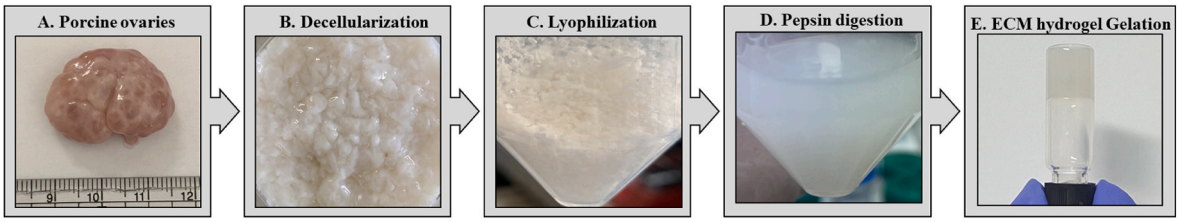

Fig. 2. Schematic diagram of the decellularization process. Decellularized ovaries were lyophilized and enzymatically digested to prepare a decellularized extracellular matrix (dECM) hydrogel for 3D culture. The pre-gel solution underwent self-assembly upon incubation at 37 °C for 30 min to induce gelation.

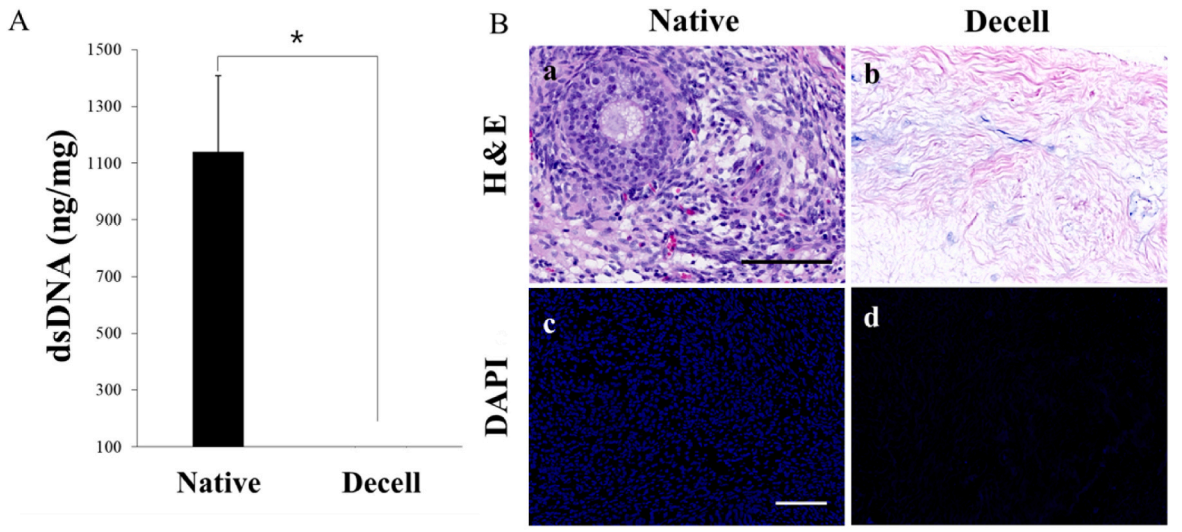

Fig. 3. DNA quantification of native and decellularized (decell) ovarian tissue. (A) The DNA contents of native and decellularized porcine ovaries were quantified. The DNA contents of the decellularized tissue were 66 ± 9.8 ng/mg (wet), which was lower by > 94 % compared to the native tissue, which was 1139 ± 269 ng/mg (wet), confirming that a significant amount of double-stranded DNA (dsDNA) was removed. Data are expressed as mean ± the standard error of the mean (SEM), *p < 0.05. Scale bar: 100μmA. (B) Hematoxylin-eosin (H&E) stained micrograph indicating basophilic (blue, nuclei) and eosinophilic (pink, cell cytoplasm and extracellular matrix) cells in native tissue (a). Basophilic staining is mostly absent, and eosinophilic staining indicates decell tissues (b). Decellularization of the ovarian tissue was confirmed by 4′,6-diamidino-2-phenylindole (DAPI) staining (c–d). (For interpretation of the references to color in this figure legend, the reader is referred to the Web version of this article.)

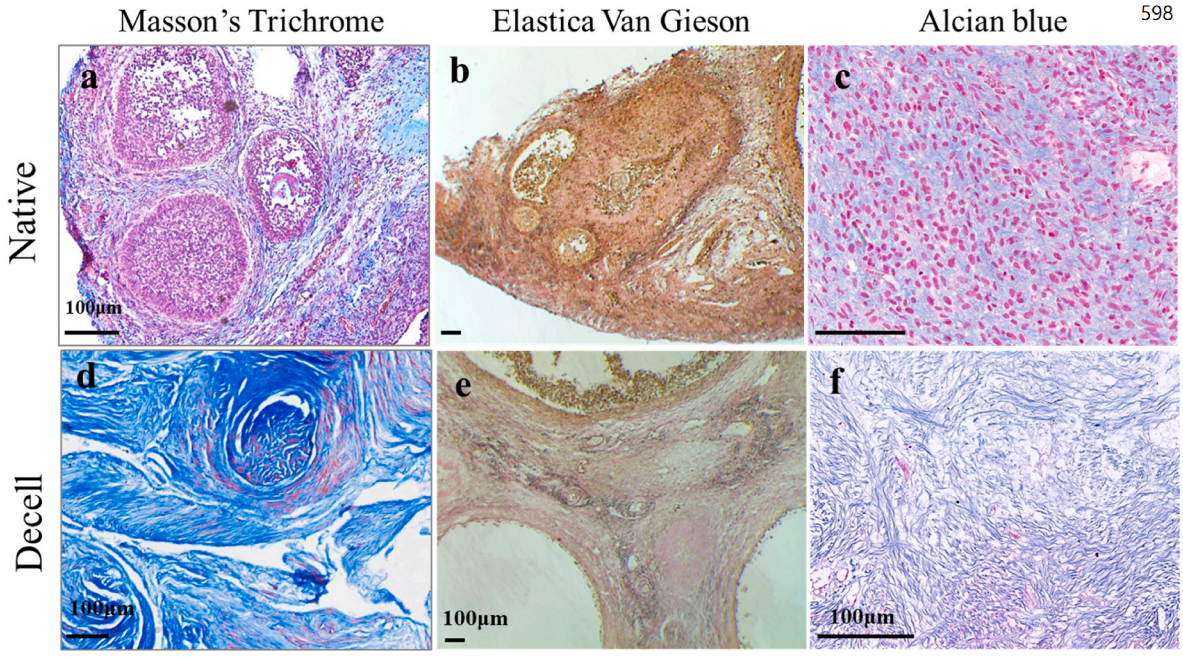

Fig. 4. Histological analysis of native and decellularized (decell) ovarian tissue. Extracellular matrix (ECM) components were analyzed by Masson's trichrome staining for collagen (a, d), Elastica Van Gieson staining for elastin (b, e), and Alcian blue staining for glycosaminoglycans (c, f). Histological images showed the persistence of ECM components between the native and Decell ovarian tissue Scale bar: 100 μm. (For interpretation of the references to color in this figure legend, the reader is referred to the Web version of this article.)

Pa, 18.9 Pa, and 49.2 Pa corresponded to the dECM hydrogel concentrations of 2, 4, and 6 mg/mL, respectively (Fig. 6B). Rheological analysis indicated a significant difference ($p < 0.05$) in mechanical strength with an increase in ECM concentration. To observe the ultrastructure of the dECM hydrogel, SEM images were obtained at different dECM hydrogel concentrations (2, 4, and 6 mg/mL). The SEM images revealed that the complex fiber network and porous structure were maintained in all groups. As the dECM hydrogel concentration increased, the space between the dECM hydrogels became narrow and compact (6 mg/mL) compared to the lower concentration of dECM hydrogel (Fig. 7).

As shown in Fig. 8, to create an optimized biomimetic ovarian environment, murine preantral follicles (2-week-old) were cultured in biomimetic ovaries with varying ECM concentrations (2, 4, and 6 mg/mL). Preantral follicles were observed on days 0, 5, 7, and 9 to measure their diameter in each of the ECM hydrogels, and it was confirmed that

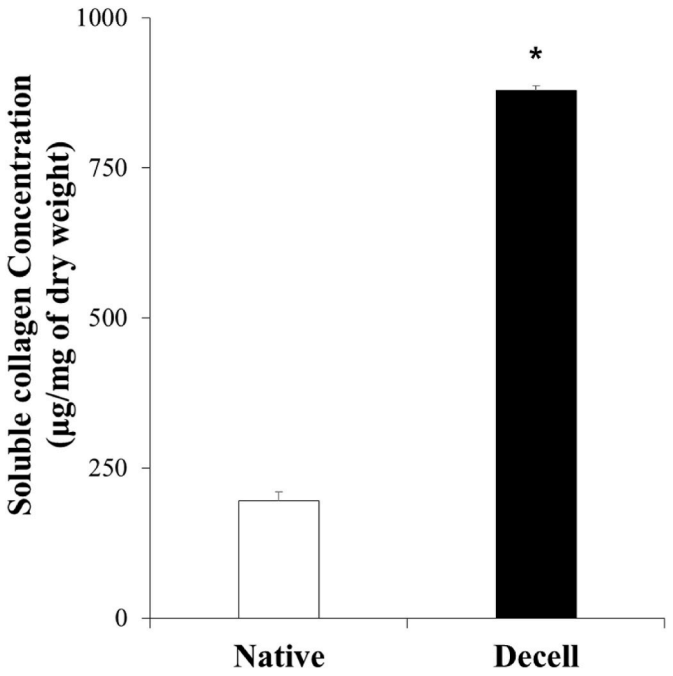

Fig. 5. Quantification of soluble collagen in decellularized ovarian tissue (decell) and native ovarian tissue (native). Concentrations of acidic-/pepsin-soluble collagen were quantified using Sircol soluble collagen.

the diameter of the preantral follicles continuously increased in all ECM hydrogels. On days 5 and 9 of culture, the dECM (4 mg/mL) group showed a significant ($p < 0.05$) increase in follicle diameter compared with the dECM hydrogel (2 and 6 mg/mL) groups. The percentage of MII oocytes retrieved from the 4 mg/mL dECM hydrogel was 47 % (50/107), which was significantly higher ($p < 0.05$) than that retrieved from the 2 and 6 mg/mL dECM hydrogels (Table 1). Follicle development and oocyte maturation were observed in biomimetic ovaries grown using ECM derived from decellularized porcine ovaries. To preserve the fertility of women diagnosed with cancer, the ovarian tissues are cryopreserved before initiating chemotherapy. After the successful treatment of cancer, ovarian tissue transplantation is performed to restore fertility in women [24]. However, the method poses a risk of tumor recurrence due to the presence of cancer cells within the tissue grafts [25]. To address this problem, using a biomimetic ovary, constructed by encapsulating ovarian follicles in dECM hydrogel to replace failed ovaries, is promising to facilitate the recovery of ovarian functions.ECM mechanical stiffness in the ovary is believed to play an essential role in regulating follicles [26–28]. When the mechanical strength of the ECM environment in the ovary is high, ovarian follicles cannot develop properly, which can lead to follicle apoptosis and a reduced proliferation rate [29,30]. The elastic modulus increased according to the dECM concentration (2, 4, and 6 mg/mL), which affected the growth of follicles in the dECM. The follicle had the weakest mechanical strength at 2 mg. The diameter of the follicle at 4 mg was the largest, whereas at 6 mg, with the strongest mechanical strength, the follicle tended to decrease in diameter. Therefore, it is important to determine the optimal mechanical properties of ECM hydrogels for use in follicle culture. However, the mechanism underlying mechanical signaling, derived from the mechanical forces of the ovary, which is involved in follicle development and oocyte maturation is not well understood [31,32]. Therefore, further studies are required to understand the role of mechanical forces on the ovary. The biomimetic ovary with dECM (4 mg/mL) may provide a suitable mechanical microenvironment to elucidate mechanism of biomechanical signals that promote follicle development and oocyte maturation.

The preantral follicles cultured in a biomimetic ovary with a decellularized porcine scaffold were better at forming antral follicles and mature oocytes than those cultured in other biomaterials, such as collagen and Matrigel. The percentage of MII oocytes retrieved from the 4 mg/mL dECM hydrogel was 27 % (26/98), which was significantly higher than that from 2.5 mg/mL collagen (Table 2). As shown in Fig. 9, follicle viability was confirmed by staining calcein-AM (live) and PI (propidium iodide, dead) in antral follicles generated by culturing for 9 days in a 4 mg/mL dECM hydrogel (Fig. 9a and b). In addition, to

A

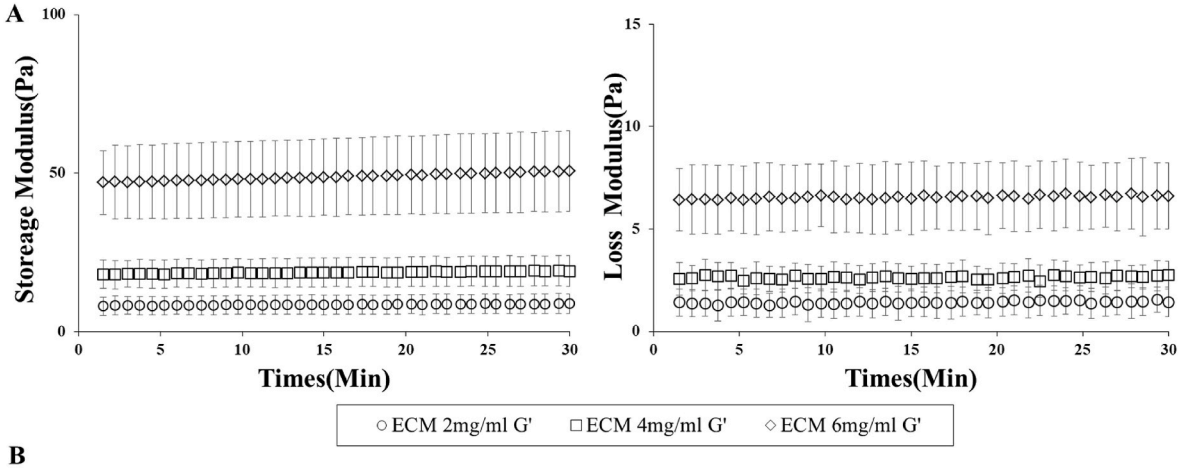

B

Rheology			
	2mg/ml	4mg/ml	6mg/ml
Storage Modulus (G';Pa)	8.5 ± 2.47	18.7 ± 3.75	48.8 ± 9.98
Loss Modulus (G",Pa)	1.4 ± 0.57	2.6 ± 0.55	6.5 ± 1.37
Elastic modulus (Pa)	8.7 ± 0.22	18.9 ± 0.33	49.2 ± 1.10

Fig. 6. Rheological characterization of extracellular matrix (ECM) hydrogels. A. The storage (G′) and loss (G″) modulus of hydrogels at ECM concentrations of 2, 4, and 6 mg/mL were determined by monitoring changes for 30 min after inducing gelation. B. Storage, loss, and elastic modulus (mean ± standard deviation [SD]) in decellularized ECM hydrogel.

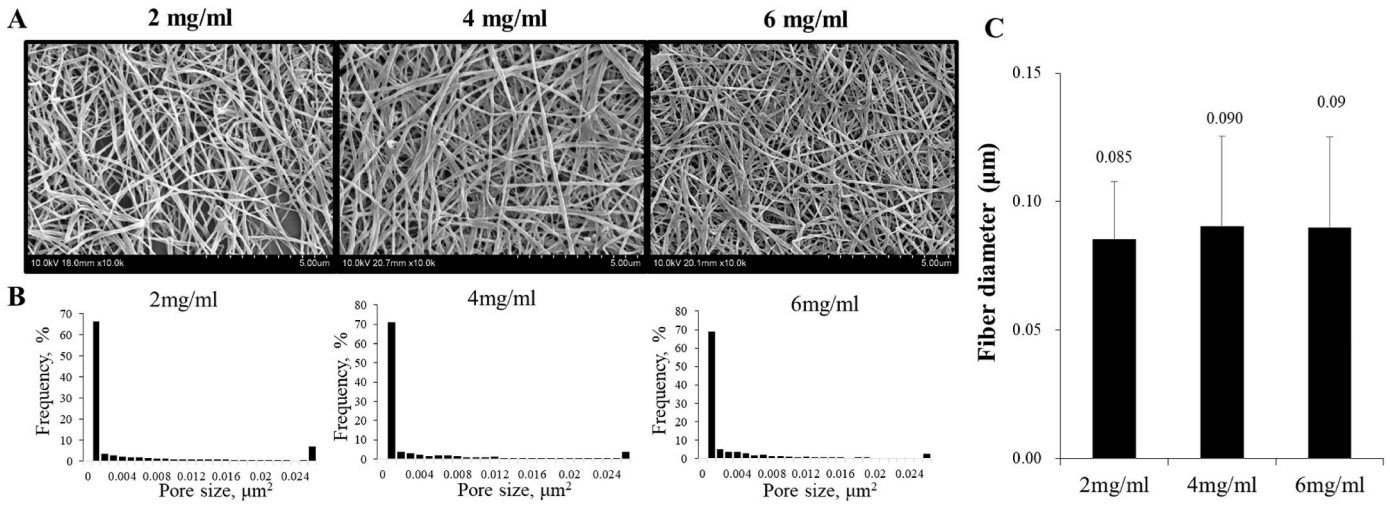

Fig. 7. Surface topology and fiber network analysis of extracellular matrix (ECM) hydrogels. Scanning electron micrographs (SEM) were obtained at 10,000 × magnification for decellularized ECM (dECM) hydrogels prepared at ECM concentrations of 2, 4, and 6 mg/mL. SEM images were analyzed using the ImageJ software to determine the average pore size (B) and fiber diameter (C) for each dECM hydrogel concentration. Scale bar for micrographs: 5 μm.

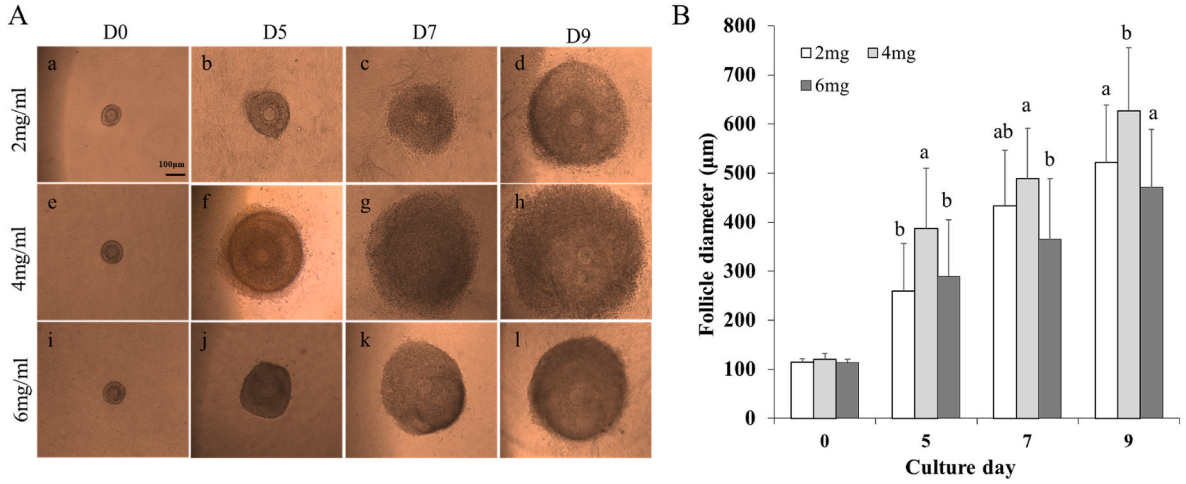

Fig. 8. In vitro development of secondary follicle of ICR mice cultured on 2, 4, 6 mg/mL ECM hydrogel. (A) Morphology of in vitro culture (IVC) in different concentrations of decellularized extracellular matrix (dECM) hydrogel ICR mice follicles at various stages of development. Secondary follicles (a,e, and i) in 2-week-old ICR mice developed to the antral stage (d,h, and l) over 9 days. (B) Follicle diameter during IVC on ECM hydrogel at different concentration from day 0 to day 9. Scale bar: 100 μm, represented data: mean ± standard deviation (SD).

Table 1
Comparison of development of pre-antral follicle cultured on 2, 4, 6 mg/mL concentration extracellular matrix (ECM) hydrogel. Data represented is from three or more independent experiments for each material.

Group	No. of follicles cultured	No. (%) of antral follicles	No. (%) of oocytes retrieved	No.[a] (%) of oocytes stage on			No. (%) of MII oocytes from follicles cultured
				GV	GVBD	MII	
ECM 2 mg/ml	93	50(54)[a]	50(54)	12 (24)	7(14)	31 (62)	31(33)[ab]
ECM 4 mg/ml	107	71(66)[a]	71(66)	4(6)	17 (24)	50 (70)	50(47)[b]
ECM 6 mg/ml	71	25(35)[b]	25(35)	1(4)	9(36)	15 (60)	15(21)[a]

GV, germinal vesicle stage; GVBD, germinal vesicle breakdown; MII, metaphase II stage.
[a] Percentage of MII oocytes out of total oocytes retrieved.
[ab] Different superscripts within the same column indicate significant differences, $P < 0.05$.

examine the chromosomal normality of MII oocytes recovered from antral follicles grown on 4 mg/mL dECM hydrogel, alpha tubulin monoclonal antibody (spindle) and Hoechst 33342 (chromosome) staining was performed (Fig. 9c and d). The follicle was stained with calcein-AM (green), indicating that it was alive, and a small number of dead cells stained with PI (red) were observed at the edge of the follicle. MII oocytes with normal spindle organization (green) and chromosomal arrangement (blue) were observed in the second meiotic metaphase.

Table 2
Comparison of oocyte retrieval from antral follicle cultured on different biomaterials. Data represented is from three or more independent experiments for each material.

Group	No. of follicles cultured	No. (%) of antral follicles	No. (%) of oocytes retrieved	No.[a] (%) of oocytes stage on			No. (%) of MII oocytes from follicles cultured
				GV	GVBD	MII	
4 mg/ml ECM	98	49(50)[a]	49(50)	10 (20)	13 (27)	26 (53)	26(27)[a]
2.5 mg/ml Collagen	107	20(19)[b]	20(19)	7(35)	1(5)	12 (60)	12(11)[b]
Matrigel	88	42(48)[a]	42(48)	9(21)	9(21)	24 (57)	24(27)[a]

GV, germinal vesicle stage; GVBD, germinal vesicle breakdown; MII, metaphase II stage.
[ab]Different superscripts within the same column indicate significant differences, $P < 0.05$.
[a] Percentage of MII oocytes out of total oocytes retrieved.

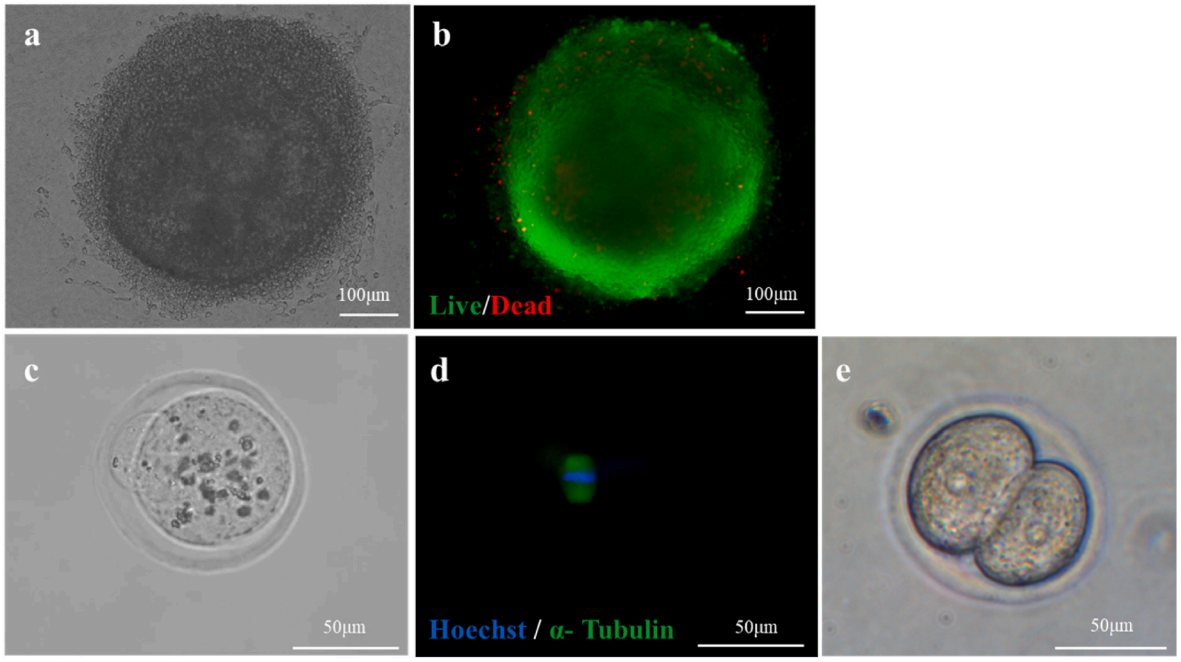

Fig. 9. Morphology of antral follicle (a–b), MII oocyte (c–d), and 2-cell embryo post-parthenogenesis (e). Immunofluorescence staining shows α-tubulin (spindle marker, green) and Hoechst (nuclei, blue) in MII oocytes (d) which appear either normal meiotic spindle organization and chromosomal alignment and antral follicle are labeled with Calcein-AM (green, live) and PI (red, dead). MII oocyte was developed into 2-cell embryos (e). (For interpretation of the references to color in this figure legend, the reader is referred to the Web version of this article.)

Mature oocytes retrieved from the 4 mg/mL dECM hydrogel developed into two-cell embryos after parthenogenetic activation (Fig. 9e), indicating that follicle development and oocyte maturation occurred normally in dECM hydrogels and matured oocytes developed into embryos.

Matrigel comprises various ECMs, such as laminin, collagen IV, entactin, heparin sulfate proteoglycan, and several growth factors extracted from Engelbreth–Holm–Swarm (EHS) mouse sarcoma [33]. It is, therefore, used to mimic the optimized 3D environment for culturing induced pluripotent stem cells [34], ovarian follicles [35], and organoids [36], as it enables the maintenance and proliferation of these cells in vitro. The 3D follicle culture using Matrigel, which is rich in ECM, cannot be directly applied to humans, as it has murine origins and carries the potential risk of animal pathogen transmission and tumorigenicity [37]. While collagen constitutes a major portion of the ECM in the ovary, it is just one component of the ECM and does not fully reflect the overall ECM composition of native ovaries. Therefore, we created a biomimetic artificial ovary that reflects the ECM environment of the entire ovary.

Biomimetic ovaries derived from the ECM isolated from decellularized porcine ovaries showed higher follicle development and more mature oocytes than those derived from Matrigel and collagen. However, there were no significant differences in antral follicle formation and mature oocytes among these biomaterials. To further demonstrate the effects of ovarian follicles in dECM, more ovarian follicle cultures are needed in the future. The use of ECM from other decellularized organs has been demonstrated to be superior to various combined biomaterials as it recapitulates the composition and bioactivity of the native organ [38,39]. Therefore, the extracellular matrix in the biomimetic ovary provides an optimal microenvironment for growing ovarian follicles and does not cause immune rejection when applied clinically because it is decellularized. Matured oocytes could be activated or fertilized to produce embryos. Therefore, we obtained 7 two-cell embryos from 16 mature oocytes following parthenogenetic activation. Compared with the in vivo ovarian microenvironment, the in vitro follicle culture system may not yet be an optimal microenvironment for folliculogenesis and oogenesis. Further studies are required to establish a culture system utilizing various growth factors, hormones, and new chemokines, so that mature oocytes derived from ovarian follicles in a biomimetic ovary can develop into blastocysts that can be implanted to produce viable offspring.

For dECM derived from various decellularized organs, in vivo safety is the most important factor for clinical applications. No adverse

immune responses were observed after dECM hydrogels were injected into the heart [40,41], liver [42], brain [43,44], lungs [45], or colon [46,47]. A biomimetic ovary was successfully established in vitro using ECM isolated from decell pig ovaries. However, an ideal decellularization protocol that can efficiently remove cellular components and nuclear materials needs to be established as standardized protocols for the decellularization of the ovary have not been fully developed. In the future, the in vivo safety of the dECM hydrogel should be confirmed after injection into the ovary for clinical application and for developing a standardized protocol for dECM in the porcine ovary.

4. Conclusions

In this study, we created a biomimetic ovary with a porcine scaffold using decellularizsation technology. Ovarian tissues were decellularized by assessing DNA content, DAPI staining, and ECM staining for collagen, GAGs, and elastin, compared to those in native tissue. We characterized the dECM hydrogels used at various concentrations (2, 4, and 6 mg/mL) by SEM and rheological analyses. The preantral follicles cultured in 4 mg/mL ECM showed high rates of antral follicle formation and mature oocyte (metaphase II) development. Preantral follicles cultured in a biomimetic ovary with a decellularized porcine scaffold were more beneficial for forming antral follicles and mature oocytes than those cultured in other biomaterials, such as collagen and Matrigel. Mature oocytes retrieved from the 4 mg/mL dECM hydrogel developed into early embryos after parthenogenetic activation. Therefore, the biomimetic ovary may contribute to fertility restoration in women with infertility and reduced ovarian function.

Ethics approval and consent to participate

All animal experiments were approved by the Animal Ethics Committee of Yeungnam University (Approval No. 2022-027).

Consent for publication

All authors agree to be published.

Funding

This research was supported by the 2019 Yeungnam University Research Grant.

Authors' contributions

E.Y.P. and J.H.P. performed all experiments (acquisition and analysis) and wrote the draft. E.Y.P., J.H.P., B.M., N.T.Q.M., and JKC conceived the study design. B.M. and J.K.C. provided the study's conceptand supervised the study. The authors read and approved the final manuscript.

CRediT authorship contribution statement

Eun young Park: Conceptualization, Methodology, Investigation, Validation, Writing – original draft. **Jin hee Park:** Conceptualization, Methodology, Investigation, Validation, Writing – original draft. **Nhu Thi Quynh Mai:** Methodology, Writing – original draft. **Byoung-San Moon:** Conceptualization, Writing – review & editing, Supervision. **Jung Kyu Choi:** Conceptualization, Writing – review & editing, Supervision.

Declaration of competing interest

The authors declare that they have no known competing financial interests or personal relationships that could have appeared to influence the work reported in this paper.

Data availability

Data will be made available on request.

Appendix A. Supplementary data

Supplementary data to this article can be found online at https://doi.org/10.1016/j.mtbio.2023.100824.

List of abbreviations

DAPI	4′,6-diamidino-2-phenylindole
decell	decellularized
dECM	decellularized extracellular matrix
dPO	decellularized porcine ovaries
ECM	extracellular matrix
EHS	Engelbreth–Holm—Swarm;
GAGs	glycosaminoglycans
H&E	hematoxylin and eosin
PA	parthenogenetic activation
SEM	scanning electron microscopy

References

[1] T. Hassold, P. Hunt, To err (meiotically) is human: the genesis of human aneuploidy, Nat. Rev. Genet. 2 (2001) 280–291, https://doi.org/10.1038/35066065.
[2] K.R. Barnett, C. Schilling, C.R. Greenfeld, D. Tomic, J.A. Flaws, Ovarian follicle development and transgenic mouse models, Hum. Reprod. Update 12 (2006) 537–555, https://doi.org/10.1093/humupd/dml022.
[3] J.R. Figueiredo, S.C.J. Hulshof, M. Thiry, R. Van den Hurk, M.M. Bevers, B. Nusgens, J.F. Beckers, Extracellular matrix proteins and basement membrane: their identification in bovine ovaries and significance for the attachment of cultured preantral follicles, Theriogenology 43 (1995) 845–858, https://doi.org/10.1016/0093-691x(95)00036-8.
[4] R.J. Rodgers, I.L. van Wezel, H.F. Irving-Rodgers, T.C. Lavranos, C.M. Irvine, M. Krupa, Roles of extracellular matrix in follicular development, J. Reprod. Fertil. Suppl. 54 (1999) 343–352, https://doi.org/10.1530/biosciprocs.4.026.
[5] M. Ramalingam, S.R. Velayudhan, Advances in induced pluripotent stem cells: nanomaterial perspectives, J. Bionanoscience 10 (2016) 163–170, https://doi.org/10.1166/jbns.2016.1339.
[6] P.K. Kreeger, J.W. Deck, T.K. Woodruff, L.D. Shea, The in vitro regulation of ovarian follicle development using alginate-extracellular matrix gels, Biomaterials 27 (2006) 714–723, https://doi.org/10.1016/j.biomaterials.2005.06.016.
[7] S. Joo, S.H. Oh, S. Sittadjody, E.C. Opara, J.D. Jackson, S.J. Lee, J.J. Yoo, A. Atala, The effect of collagen hydrogel on 3D culture of ovarian follicles, Biomed. Mater. 11 (2016), 065009, https://doi.org/10.1088/1748-6041/11/6/065009.
[8] A. Shikanov, M. Xu, T.K. Woodruff, L.D. Shea, Interpenetrating fibrin–alginate matrices for in vitro ovarian follicle development, Biomaterials 30 (2009) 5476–5485, https://doi.org/10.1016/j.biomaterials.2009.06.054.
[9] J.E. Ihm, S.T. Lee, D.K. Han, J.M. Lim, J.A. Hubbell, Murine ovarian follicle culture in PEG-hydrogel: effects of mechanical properties and the hormones FSH and LH on development, Macromol. Res. 23 (2015) 377–386, https://doi.org/10.1007/s13233-015-3045-x.
[10] J.I. Ahn, G.A. Kim, H.S. Kwon, J.Y. Ahn, J.A. Hubbell, Y.S. Song, S.T. Lee, J.M. Lim, Culture of preantral follicles in poly(ethylene) glycol-based, three-dimensional hydrogel: a relationship between swelling ratio and follicular developments, J. Tissue Eng. Regen. Med. 9 (2015) 319–323, https://doi.org/10.1002/term.1824.
[11] E.E. Telfer, M.B. Zelinski, Ovarian follicle culture: advances and challenges for human and nonhuman primates, Fertil. Steril. 99 (2013) 1523–1533, https://doi.org/10.1016/j.fertnstert.2013.03.043.
[12] W.Y. Liu, S.G. Lin, R.Y. Zhuo, Y.Y. Xie, W. Pan, X.F. Lin, F.X. Shen, Xenogeneic decellularized scaffold: a novel platform for ovary regeneration, Tissue Eng, Part C Methods 23 (2017) 61–71, https://doi.org/10.1089/ten.TEC.2016.0410.
[13] A.B. Alshaikh, A.M. Padma, M. Dehlin, R. Akouri, M.J. Song, M. Brännström, M. Hellström, Decellularization of the mouse ovary: comparison of different scaffold generation protocols for future ovarian bioengineering, J. Ovarian Res. 12 (2019) 58, https://doi.org/10.1186/s13048-019-0531-3.
[14] K. Gutierrez, N. Dicks, W.G. Glanzner, L.B. Agellon, V. Bordignon, Efficacy of the porcine species in biomedical research, Front. Genet. 6 (2015) 293, https://doi.org/10.3389/fgene.2015.00293.
[15] M. Kulus, P. Sujka-Kordowska, A. Konwerska, P. Celichowski, W. Kranc, J. Kulus, H. Piotrowska-Kempisty, P. Antosik, D. Bukowska, D. Iżycki, M. Bruska, M. Zabel, M. Nowicki, B. Kempisty, New molecular markers involved in regulation of ovarian granulosa cell morphogenesis, development and differentiation during short-term primary in vitro culture–Transcriptomic and histochemical study based on ovaries and individual separated follicles, Int. J. Mol. Sci. 20 (2019) 3966, https://doi.org/10.3390/ijms20163966.

[16] M.T. Wolf, K.A. Daly, E.P. Brennan-Pierce, S.A. Johnson, C.A. Carruthers, A. D'Amore, S.P. Nagarkar, S.S. Velankar, S.F. Badylak, A hydrogel derived from decellularized dermal extracellular matrix, Biomaterials 33 (2012) 7028–7038, https://doi.org/10.1016/j.biomaterials.2012.06.051.
[17] A. D'Amore, J.A. Stella, W.R. Wagner, M.S. Sacks, Characterization of the complete fiber network topology of planar fibrous tissues and scaffolds, Biomaterials 31 (2010) 5345–5354, https://doi.org/10.1016/j.biomaterials.2010.03.052.
[18] M. Lebbe, A.E. Taylor, J.A. Visser, J.C. Kirkman-Brown, T.K. Woodruff, W. Arlt, The steroid metabolome in the isolated ovarian follicle and its response to androgen exposure and antagonism, Endocrinology 158 (2017) 1474–1485, https://doi.org/10.1210/en.2016-1851.
[19] H.G. Vogel, Collagen and mechanical strength in various organs of rats treated with D-penicillamine or amino-acetonitrile, Connect. Tissue Res. 3 (1975) 237–244, https://doi.org/10.3109/03008207509152184.
[20] W. Zhang, Y. Liu, H. Zhang, Extracellular matrix: an important regulator of cell functions and skeletal muscle development, Cell Biosci. 65 (2021), https://doi.org/10.1186/s13578-021-00579-4.
[21] S.R. Caliari, J.A. Burdick, A practical guide to hydrogels for cell culture, Nat. Methods 13 (2016) 405–414, https://doi.org/10.1038/nmeth.3839.
[22] Y.E. Arslan, Y.F. Galata, T.S. Arslan, B. Derkus, Trans-differentiation of human adipose-derived mesenchymal stemcells into cardiomyocyte-like cells on decellularized bovine myocardial extracellular matrix-based films, J. Mater. Sci. Mater. Med. 29 (2018) 127.
[23] T.K. Woodruff, L.D. Shea, The role of the extracellular matrix in ovarian follicle development, Reprod. Sci. 14 (2007) 6–10, https://doi.org/10.1177/1933719107309818.
[24] S. Kim, Y. Lee, S. Lee, T. Kim, Ovarian tissue cryopreservation and transplantation in patients with cancer, Obstet Gynecol Sci 61 (2018) 431–442, https://doi.org/10.5468/ogs.2018.61.4.431.
[25] T.Y.T. Nguyen, A. Camboni, R. Masciangelo, J. Donnez, M.-M. Dolmans, Is ovarian tissue transplantation safe in patients with central nervous system primitive neuroectodermal tumors? J. Clin. Med. 9 (2020) 4101, https://doi.org/10.3390/jcm9124101.
[26] J.S. Shah, R. Sabouni, K.C. Cayton Vaught, C.M. Owen, D.F. Albertini, J.H. Segars, Biomechanics and mechanical signaling in the ovary: a systematic review, J. Assist. Reprod. Genet. 35 (2018) 1135–1148, https://doi.org/10.1007/s10815-018-1180-y.
[27] E. Ouni, A. Peaucelle, K.T. Haas, O. Van Kerk, M.M. Dolmans, T. Tuuri, M. Otala, C. A. Amorim, A blueprint of the topology and mechanics of the human ovary for next-generation bioengineering and diagnosis, Nat. Commun. 12 (2021) 5603, https://doi.org/10.1038/s41467-021-25934-4.
[28] T.I.R. Hopkins, V.L. Bemmer, S. Franks, C. Dunlop, K. Hardy, I.E. Dunlop, Micromechanical mapping of the intact ovary interior reveals contrasting mechanical roles for follicles and stroma, Biomaterials 12 (2021), 121099, https://doi.org/10.1016/j.biomaterials.2021.121099.
[29] J.K. Choi, P. Agarwal, H. Huang, S. Zhao, X. He, The crucial role of mechanical heterogeneity in regulating follicle development and ovulation with engineered ovarian microtissue, Biomaterials 35 (2014) 5122–5128, https://doi.org/10.1016/j.biomaterials.2014.03.028.
[30] F. Fàbregues, J. Ferreri, M. Méndez, J.M. Calafell, J. Otero, R. Farré, In vitro follicular activation and stem cell therapy as a novel treatment strategies in diminished ovarian reserve and primary ovarian insufficiency, Front. Endocrinol. 11 (2020), 617704, https://doi.org/10.3389/fendo.2020.617704.
[31] S. Jorge, S. Chang, J.J. Barzilai, P. Leppert, J.H. Segars, Mechanical signaling in reproductive tissues: mechanisms and importance, Reprod. Sci. 21 (2014) 1093–1107, https://doi.org/10.1177/1933719114542023.
[32] J.T. Thorne, T.R. Segal, S. Chang, S. Jorge, J.H. Segars, P.C. Leppert, Dynamic reciprocity between cells and their microenvironment in reproduction, Biol. Reprod. 92 (2015) 25, https://doi.org/10.1095/biolreprod.114.121368.
[33] H.K. Kleinman, M.L. McGarvey, J.R. Hassell, V.L. Star, F.B. Cannon, G.W. Laurie, G.R. Martin, Basement membrane complexes with biological activity, Biochemistry 30 (1986) 312–328, https://doi.org/10.1021/bi00350a005.
[34] M.T. Lam, M.T. Longaker, Comparison of several attachment methods for human iPS, embryonic and adipose-derived stem cells for tissue engineering, J. Tissue Eng. Regen. Med. 6 (S 3) (2012) s80–s86, https://doi.org/10.1002/term.1499.
[35] C.M. Higuchi, Y. Maeda, T. Horiuchi, Y. Yamazaki, A simplified method for three-dimensional (3-D) ovarian tissue culture yielding oocytes competent to produce full-term offspring in mice, PLoS One 10 (2015), e0143114, https://doi.org/10.1371/journal.pone.0143114.
[36] S. Kim, S. Min, Y.S. Choi, S.H. Jo, J.H. Jung, K. Han, J. Kim, S. An, Y.W. Ji, Y. G. Kim, S.W. Cho, Tissue extracellular matrix hydrogels as alternatives to Matrigel for culturing gastrointestinal organoids, Nat. Commun. 13 (2022) 1692, https://doi.org/10.1038/s41467-022-29279-4.
[37] O. Habanjar, M. Diab-Assaf, F. Caldefie-Chezet, L. Delort, 3D cell culture systems: tumor application, advantages, and disadvantages, Int. J. Mol. Sci. 22 (2021), 12200, https://doi.org/10.3390/ijms222212200.
[38] Y.S. Kim, M M, A.J. Melchiorri, A.G. Mikos, Applications of decellularized extracellular matrix in bone and cartilage tissue engineering, Bioeng Transl Med 4 (2019) 83–95, https://doi.org/10.1002/btm2.10110.
[39] M. Brown, J. Li, C. Moraes, M. Tabrizian, N.Y.K. Li-Jessen, Decellularized extracellular matrix: new promising and challenging biomaterials for regenerative medicine, Biomaterials 289 (2022), 121786, https://doi.org/10.1016/j.biomaterials.2022.121786.
[40] S.B. Seif-Naraghi, M.A. Salvatore, P.J. Schup-Magoffin, D.P. Hu, K.L. Christman, Design and characterization of an injectable pericardial matrix gel: a potentially autologous scaffold for cardiac tissue engineering, Tissue Eng. 16 (2010) 2017–2027, https://doi.org/10.1089/ten.TEA.2009.0768.
[41] T.D. Johnson, J.A. DeQuach, R. Gaetani, J. Ungerleider, D. Elhag, V. Nigam, A.B.K. L. Christman, Human versus porcine tissue sourcing for an injectable myocardial matrix hydrogel, Biomater. Sci. 2 (2014) 735–744, https://doi.org/10.1039/C3BM60283D.
[42] J.S. Lee, J. Shin, H.M. Park, Y.G. Kim, B.G. Kim, J.W. Oh, S.W. Cho, Liver extracellular matrix providing dual functions of two-dimensional substrate coating and three-dimensional injectable hydrogel platform for liver tissue engineering, Biomacromolecules 15 (2014) 206–218, https://doi.org/10.1021/bm4015039.
[43] H. Ghuman, A.R. Massensini, J. Donnelly, S.M. Kim, C.J. Medberry, S.F. Badylak, M. Modo, ECM hydrogel for the treatment of stroke: characterization of the host cell infiltrate, Biomaterials 91 (2016) 166–181, https://doi.org/10.1016/j.biomaterials.2016.03.014.
[44] A.R. Massensini, H. Ghuman, L.T. Saldin, C.J. Medberry, T.J. Keane, F.J. Nicholls, S.S. Velankar, S.F. Badylak, M. Modo, Concentration-dependent rheological properties of ECM hydrogel for intracerebral delivery to a stroke cavity, Acta Biomater. 27 (2015) 116–130, https://doi.org/10.1016/j.actbio.2015.08.040.
[45] R.A. Pouliot, P.A. Link, N.S. Mikhaiel, M.B. Schneck, M.S. Valentine, F.J. Kamga Gninzeko, J.A. Herbert, M. Sakagami, R.L. Heise, Development and characterization of a naturally derived lung extracellular matrix hydrogel, J. Biomed. Mater. Res. A. 104 (2016) 1922–1935, https://doi.org/10.1002/jbm.a.35726.
[46] T.J. Keane, J. Dziki, E. Sobieski, A. Smoulder, A. Castleton, N. Turner, et al., Restoring mucosal barrier function and modifying macrophage phenotype with an extracellular matrix hydrogel: potential therapy for ulcerative colitis, J Crohn's Colitis. 11 (2017) 360–368, https://doi.org/10.1093/ecco-jcc/jjw149.
[47] T.J. Keane, J. Dziki, A. Castelton, D.M. Faulk, V. Messerschmidt, R. Londono, J. E. Reing, S.S. Velankar, S.F. Badylak, Preparation and characterization of a biologic scaffold and hydrogel derived from colonic mucosa, J. Biomed. Mater. Res. B Appl. Biomater. 105 (2017) 291–306, https://doi.org/10.1002/jbm.b.33556.